KINETICS, CATALYSIS, AND REACTION ENGINEERING

A Study about the Propane Ammoxidation to Acrylonitrile with an Alumina-Supported Sb−V−O Catalyst

M. Olga Guerrero-Pérez,*,† Miguel A. Peña, J. L. G. Fierro, and Miguel A. Bañares*

Instituto de Catálisis y Petroleoquímica, CSIC, Marie Curie 2, E-28049 Madrid, Spain

The propane ammoxidation reaction is investigated on an alumina-supported Sb−V−O catalyst with an Sb/V atomic ratio of 1 at nominal Sb + V monolayer coverage on alumina support. The roles of reaction temperature and of the partial pressure of reactants in the reaction are evaluated. Fresh and used catalyst is characterized by X-ray diffraction, Raman spectroscopy, and X-ray photoelectron spectroscopy. The effect of sudden changes in reaction feed is used to understand if the transient activation of the catalysts during the first hours on-stream is due to surface intermediates or to a change in the catalyst structure. A discussion is presented about the reaction network and the nature of the active phases.

Introduction

Nitriles such as acrylonitrile have been industrially produced as important intermediates for the preparation of fibers, synthetic resins, synthetic rubbers, and the like.[1,2] Acrylonitrile production has increased linearly during the last 4 decades,[3] and the direct conversion of propane into acrylonitrile is an alternative route to the conventional propylene ammoxidation. The economic implications of this new route are very important since propylene is more expensive than propane.[1] Thus, in 1997 British Petroleum started a demonstration plant to make acrylonitrile, using propane, and estimated to decrease production costs ca. 20% compared with conventional propylene-based technology.[4] In this reaction, the activation of propane is the limiting step.[1,5] Since the adsorption rate of propane is near 10 times smaller than that of propylene,[6] the conversion of propane is at least 10 times smaller than that of propylene.[7] The reaction conditions to activate the C−H bond in propane are more energy demanding, which has a negative effect on selectivity. The use of homogeneous−heterogeneous processes to promote propane to propylene conversion upstream from the catalyst bed is an option.[8] However, other side reactions may take place in the gas phase, like ammonia oxidation to nitrogen in the presence of molecular oxygen.[9] The low activity of propane has also led to the use of gas-phase additives (e.g., H_2S or CH_3Br) as radical generators (see ref 9 and references therein). However, environmental concerns do not make this option attractive. Therefore, the efforts focus on a catalyst for the direct ammoxidation of propane into acrylonitrile with no additives in the gas phase.

Different catalytic systems have been investigated for the ammoxidation of propane into acrylonitrile, and Sb−V-based catalysts have been found to be one of the most promising,[1,5,9−14] especially, the Sb−V−Al system.[13,15−18] Several studies about the mechanism of ammoxidation over this Sb−V catalyst system have been made, and propylene is commonly proposed as the first intermediate,[5,19−22] but the details on the reaction mechanism and the influence of feed composition and the structure of the catalyst are not fully understood. Some systems appear to possess suprasurface Sb species on top of V−Sb oxide,[1,16,23−25] whereas other systems are reported to possess a surface excess of vanadium.[13]

Previous contributions showed that Sb−V−O-supported catalysts on Al_2O_3 and Nb_2O_5 are active and selective for this reaction, in particular, when the Sb/V atomic ratio is near 1.[3,18,26,27] The present paper studies the direct ammoxidation of propane on an alumina-supported catalyst with Sb/V = 1 prepared with a soluble Sb precursor, evaluates the role of the reactants, reaction temperature and time on-stream, and discusses the nature of the active sites.

Experimental Section

The alumina-supported Sb−V−O catalyst was prepared adding a soluble antimony tartrate complex[28] to an aqueous solution of NH_4VO_3 (Sigma); this solution was kept under stirring at 80 °C for 50 min, and then γ-Al_2O_3 (Girdler Süd-Chemie) was added. The resulting dispersion was dried in a rotatory evaporator at 80 °C. The resulting solid was dried at 115 °C for 24 h, obtaining the catalyst precursor. This precursor was calcined at 400 °C for 4 h. Sb/V atomic ratio was fixed at 1, and the total coverage of V + Sb would correspond to 100% of its nominal dispersion limit. The dispersion limit is understood as the maximum surface loading of V + Sb units that remain dispersed, free of crystalline phase (e.g., V_2O_5, Sb_2O_3, α-Sb_2O_4 or $SbVO_4$), as observed by Raman spectroscopy. $VSbO_4$ is not stable if V + Sb loading is below such coverage on alumina.[18] The dispersion limit for Sb−V oxides on alumina is ca. 9 atoms/nm^2. The absence of $VSbO_4$ on alumina results in a catalyst containing surface vanadia and antimony species that is not efficient for propane ammoxidation.[18]

Nitrogen adsorption isotherms (−196 °C) were recorded on an automatic Micromeritics ASAP-2000 apparatus. Prior to the adsorption experiments, samples were outgassed at 140 °C for 2 h. BET areas were computed from the adsorption isotherms ($0.05 < P/P_0 < 0.27$), taking a value of 0.164 nm^2 for the cross-

* To whom correspondence should be addressed. Fax: +34915854760. Tel.: +34915854879. E-mail: banares@icp.csic.es.

† Present address: Departamento de Ingeniería Química, Universidad de Málaga, E-29071 Málaga, Spain.

10.1021/ie051000g CCC: $33.50
Published on Web 05/19/2006

section of the adsorbed N_2 molecule at −196 °C. X-ray diffraction patterns were recorded on a Siemens Krystalloflex D-500 diffractometer using Cu Kα radiation ($\lambda = 0.154\,18$ nm) and a graphite monochromator. Working conditions were 40 kV and 30 mA and a scanning rate of 2°/min for Bragg's angles (2θ) from 5 to 70°.

Raman spectra were acquired with a single monochromator Renishaw System 1000 equipped with a cooled CCD detector (−73 °C) fitted with a holographic super-Notch filter. Such filter removes the elastic scattering, and the Raman signal remains higher than when triple monochromator spectrometers are used. The samples were excited with the 514 nm Ar line; spectral resolution was ca. 3 cm^{-1}, and spectrum acquisition consisted of 20 accumulations of 30 s. The spectra were obtained under dehydrated conditions (200 °C, after pretreatment at 400 °C during 1 h) in a hot stage (Linkam TS-1500).

XPS measurements were performed using a VG Escalab 200 R electron spectrometer, equipped with a twin Mg/Al anode as X-ray source and a hemispherical electron analyzer. The spectra were recorded at constant analyzer energy (CAE) mode, using a pass energy of 20 eV. Typical base pressure was maintained in the range of 10^{-8} mbar. The charging effect of the samples was corrected by referring the spectra to the Al 2p line at 74.2 eV. Nonmonochromatic Al Kα radiation (mean line at 1486.6 eV) was used, operated at 12 kV and 10 mA. The use of this radiation avoids the interaction of V 2p lines with the Sb MNN Auger line, which happens if Mg Kα radiation is used. Atomic surface ratio were obtained using the area under the curve of lines Sb $3d_{3/2}$ (assuming a 3:2 intensity ratio of $3d_{5/2}$:$3d_{3/2}$), V $2p_{3/2}$, and Al 2p, with the atomic sensitivity factors reported by Wagner et al.[29] Curve fitting was done considering a Shirley-type background. An imposed 1:2 intensity ratio was used for fitting V $2p_{1/2}$:V $2p_{3/2}$ lines. O 1s and Sb $3d_{5/2}$ satellites (present when nonmonochromatic radiation is used) fall in the V 2p region, and their contribution were taken into account when lines in this region were fitted.

Activity measurements were performed using a conventional microreactor with on-line gas chromatograph, equipped with a flame ionization and thermal-conductivity detector and with a Porapak Q column and Molecular Sieve. The correctness of the analytical determinations was checked for each test by verification that the carbon balance (based on the propane converted) was within the cumulative mean error of the determinations (±10%). Yields and selectivities in products were determined on the basis of the moles of propane feed and products, considering the number of carbon atoms in each molecule. To prevent participation of homogeneous reaction,[8] the reactor was designed to minimize gas-phase activation upstream and downstream the catalyst bed and was made of quartz. Upstream the catalyst bed, the reactor consisted of a 9 mm o.d. (7 mm i.d.) quartz tube and an inside closed 6 mm o.d. quartz tube. Downstream the catalyst bed, the reactor consisted of a capillary 6 mm o.d. (2 mm i.d.) quartz tube. The axial temperature profile was monitored by a thermocouple sliding inside the closed 6 mm o.d. quartz tube inserted into the catalytic bed. The total flow rate was 20 mL/min corresponding to a gas-space velocity (GHSV) of 3000 h^{-1}. The reaction feed consisted of propane, ammonia, oxygen, and helium. The effect of the partial pressure of each reactant was evaluated, keeping the partial pressure of the other reactants constant while He was used to compensate.

Internal diffusion phenomena were evaluated for propane ammoxidation with catalyst particle size ranging from 1.00 to 0.05 mm.[30] The particle size range of 0.250−0.125 mm showed no internal diffusion. External diffusion phenomena were studied for propane ammoxidation at different total flows (F) of reactant at constant GHSV, using particle dimensions in the 0.250−0.125 mm range.[30] No external diffusion problems are present for 0.20 g of catalyst using a total flow of 20 mL/min. So, tests were made using 0.20 g of sample with particle dimensions in the 0.250−0.125 mm range.

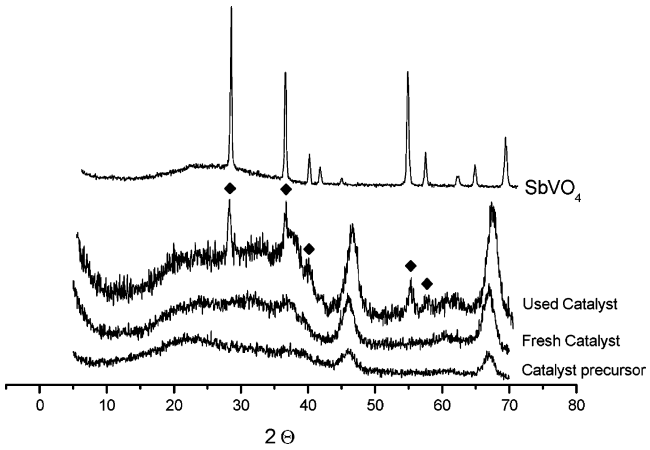

Figure 1. XRD patterns of fresh and used catalyst, catalyst precursor, and reference $SbVO_4$ phase.

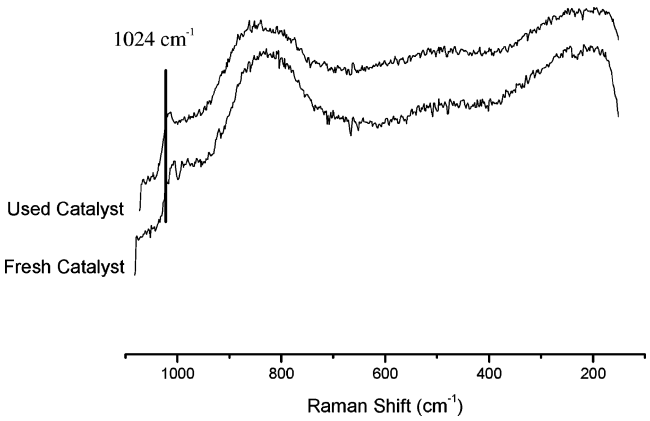

Figure 2. Raman spectra of fresh and used dehydrated catalyst.

Results

Bulk and Surface Characterization of Catalyst. The BET area for the γ-Al_2O_3 support is 160 m^2/g; the V−Sb−O/Al_2O_3 catalyst BET area is 140 m^2/g. Nominal composition of catalyst was confirmed by ICP elemental chemical analysis (9.4% Sb, 3.8% V).

Figure 1 shows the X-ray diffraction (XRD) patterns of reference $VSbO_4$, fresh and used catalyst, and its precursor. The diffraction patterns of the fresh catalyst and its precursor are quite similar and correspond to alumina support. The used catalyst shows new weak features that correspond to $SbVO_4$ (JCPDS 16-0600). Figure 2 shows the Raman spectra of the fresh and used dehydrated catalysts. Both samples exhibit the same Raman bands: the Raman band at 1024 cm^{-1}, sensitive to hydration, characteristic of surface VO_x species,[31] and a broad band centered at 800 cm^{-1} characteristic of $SbVO_4$ phase.[16] Sb_2O_3 and α-Sb_2O_4 exhibit intense Raman bands,[18] which are not observed in these catalysts.

The XP spectra of fresh and used catalysts are shown in Figure 3, corresponding to the Sb 3d−O 1s−V 2p region. Since O 1s and Sb $3d_{5/2}$ peaks are superimposed, only Sb $3d_{3/2}$ was used for quantification. The O 1s + Sb $3d_{5/2}$ satellite line is

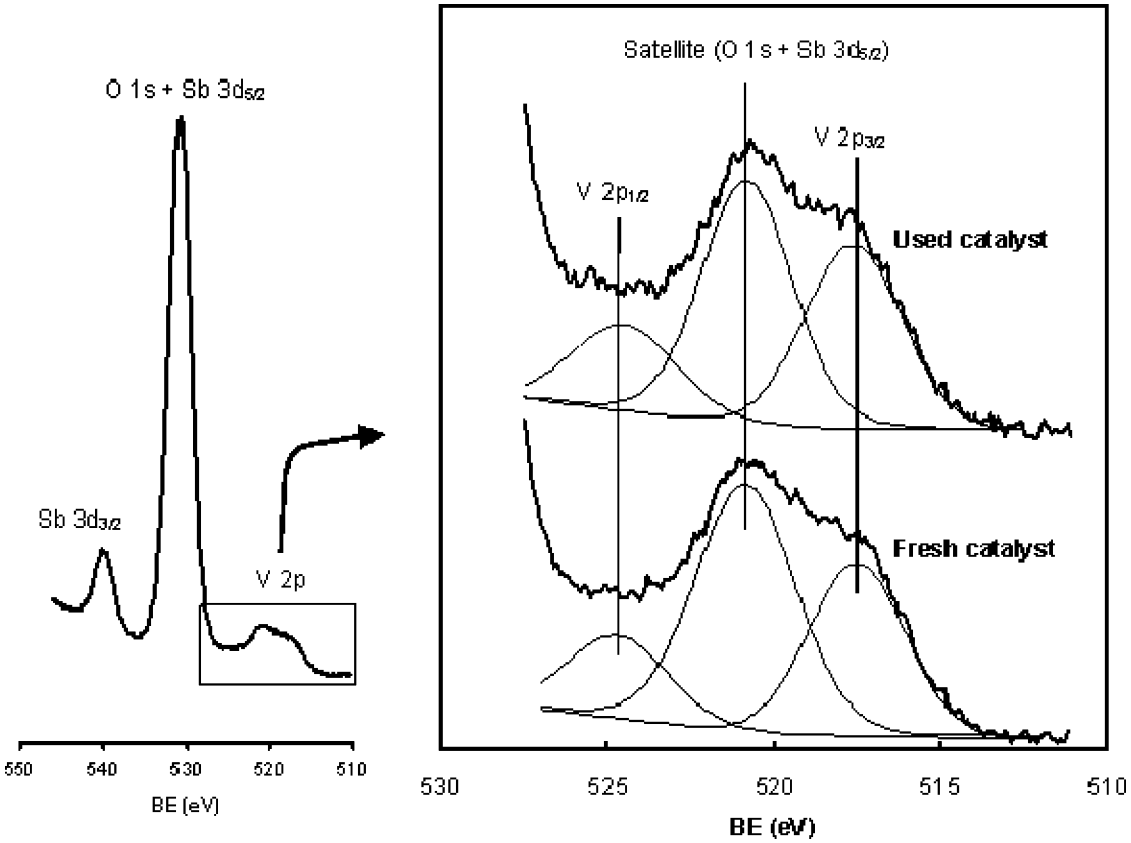

Figure 3. XPS spectra of catalyst in the Sb 3d−O 1s−V 2p region and detail of the V 2p region for the fresh and used catalyst.

Table 1. Binding Energies (eV) and XPS Surface Atomic Ratio of Fresh and Used Catalysts

	binding energy (eV)			XPS surface atomic ratio	
	V $2p_{3/2}$	V $2p_{1/2}$	Sb $3d_{3/2}$	V/Sb	Al/(Sb + V)
fresh catalyst	517.5	524.7	539.8	1.0	5.2
used catalyst	517.6	524.5	539.8	1.0	4.6

considered in order to fit the V 2p lines (Figure 3, right panel). Table 1 summarizes the XPS data. The BE value of V $2p_{3/2}$ line (517.5 eV) is characteristic of V^{5+} species in V−Sb−O-based systems,[16,23,24,32−34] typically above 517.0 eV. The bulk $VSbO_4$ phase possesses V^{3+} species that must be oxidized at the outermost layer since V species in $VSbO_4$ possesses a very dynamic redox character.[23,35] The high value of the BE for the V $2p_{3/2}$ line implies that all surface vanadium is in its higher oxidation state, as it has been reported for other alumina-supported Sb−V−O system.[23] Unsupported oxides have a different behavior, and, in addition to V^{5+}, other lower oxidation states ($V^{4+/3+}$) can be found.[13,16,23,24,32−34] The V 2p spectra of the fresh and used catalysts show no appreciable differences in the V $2p_{3/2}$ BE (517.6 eV) or in the full width at half-maximum (fwhm) value. The stability of the oxidation state of surface vanadium after reaction was also reported by Nilsson et at.[16] On the contrary, Zanthoff et al.[13] describe the reduction of part of the surface V^{5+} to V^{4+}, and a similar trend is observed during the ODH of isobutane in nonsupported Sb−V−O catalysts.[23] The BE value for Sb $3d_{3/2}$ in the fresh catalyst is 539.8 eV. This BE value is close to that of the Sb^{5+} species[16,23−25,32−34] in V−Sb−O-based systems, but the presence of some proportion of Sb^{3+} sites cannot be ruled out[16,24,25,33,34] due to the little difference in BE between both Sb oxidation states (ca. 0.8 eV). After reaction, no appreciable shift in the BE (539.8 eV) or in the fwhm values is observed. This stability under reaction

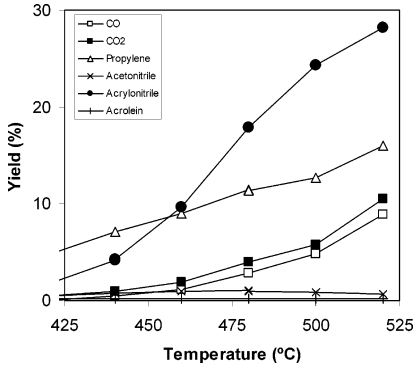

Figure 4. Yields to principal reaction products as a function of the reaction temperature for the Sb−V−Al−O catalyst. Reaction conditions: total flow, 20 mL/min; feed composition (% volume), $C_2H_8/O_2/NH_3$ (9.8/25/8.6), 200 mg of catalyst.

conditions of the oxidation state of Sb has been previously described in the Sb−V−O system after reaction.[16,23]

Catalytic Tests. The steady-state yields to different products as a function of the reaction temperature are illustrated in Figure 4. At low temperatures, propylene is the main product, while acrylonitrile becomes the main product if the reaction temperature is higher than 460 °C. As the temperature increases, CO_x yield also increases due to combustion. Figure 5 illustrates the selectivity−conversions profiles for acrylonitrile, CO, CO_2, propylene, acetonitrile, and acrolein. For a given temperature, the selectivity to propylene, acetonitrile, and acrolein decreases continuously. At low propane conversion, the main product is propylene. At medium conversions (between 20 and 60%) acrylonitrile is the main product. At conversions higher than 60% the CO_x is the main product.

Figure 6 shows the effect of the partial pressures of oxygen, ammonia, and propane on the ammoxidation reaction during

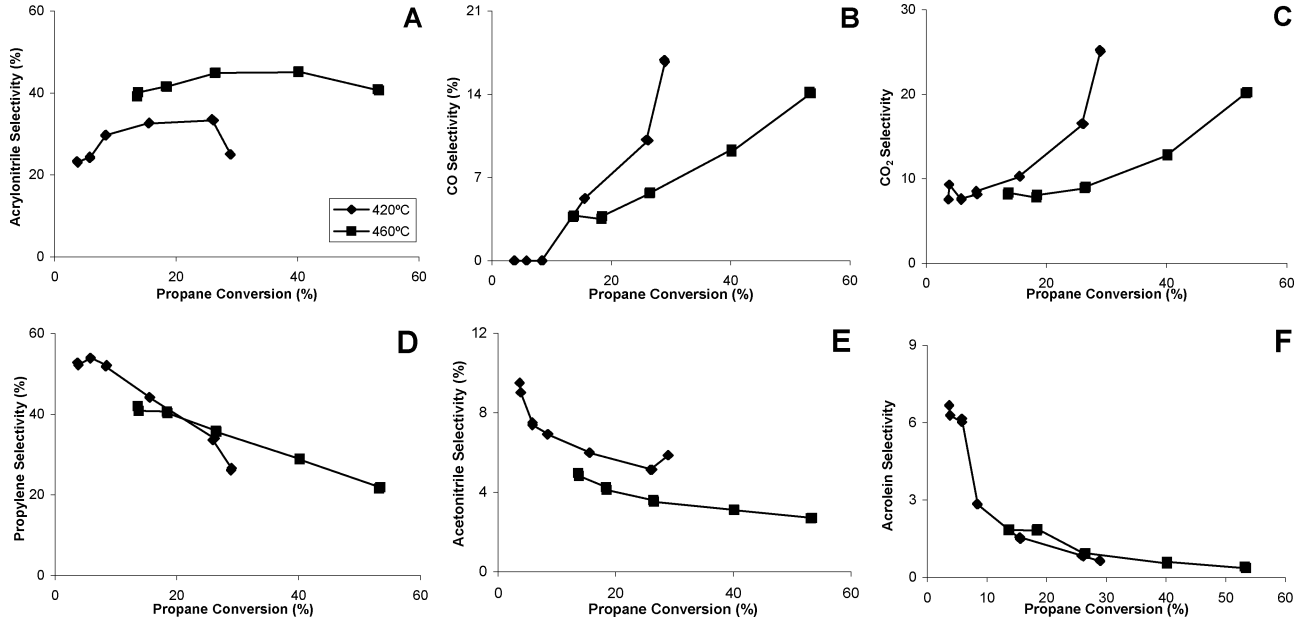

Figure 5. Selectivity−conversion profiles for acrylonitrile (A), CO (B), CO_2 (C), propylene (D), acetonitrile (E), and acrolein (F) at different reaction conditions. Reaction conditions: total flow was changed between 3 and 40 mL/min; feed composition (% volume), $C_2H_8/O_2/NH_3$ (9.8/25/8.6), 200 mg of catalyst.

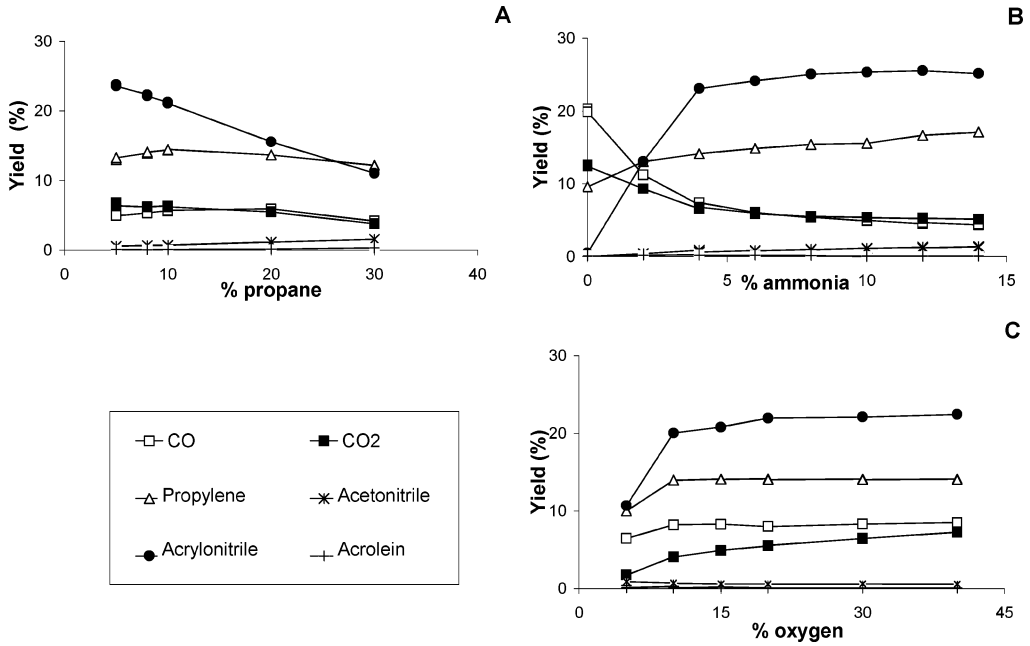

Figure 6. Yields to different products versus percentage of propane (A), ammonia (B), and oxygen (C). Reaction conditions: total flow, 20 mL/min; feed composition (% volume), $C_2H_8/O_2/NH_3$ (9.8/25/8.6), 200 mg of catalyst. Reaction temperature: 500 °C.

steady-state operation. The effect of propane concentration in the feed is represented in Figure 6A. When propane concentration increases, the yield to acrylonitrile decreases linearly and the yield to propylene remains essentially constant.

Figure 6B shows the effect of ammonia partial pressure. When no ammonia is in the feed, CO_x products dominate due to nonselective oxidation of propane. When ammonia concentration increases, the yields to acrylonitrile and propylene increase while the yields to CO_x decrease. This effect of ammonia levels off above 7% NH_3. Figure 6C shows the effect of oxygen concentration. The reaction is limited at the lowest oxygen concentrations, where oxygen reaches total conversion. Propylene and acrylonitrile are the main products at low O_2 concentration, while CO_x production increases at higher oxygen concentration values.

The Sb−V−Al−O catalyst was tested during time on-stream for 20 h at 500 °C (Figure 7). Acrylonitrile and propylene yields increase moderately during the first hours of reaction thus increasing propane conversion. Apparently, the product distribution is not significantly affected, unlike most Sb−V−O catalysts; this may indicate that the nature of the active phase is not affected. In the absence of ammonia, combustion, and propane oxidative dehydrogenation are the main reactions. When ammonia feed is restored, the yields to all the products return to the values prior to ammonia cutoff.

Discussion

Characterization of Catalyst. $SbVO_4$ phase is present in fresh and used catalysts as it was visible by Raman spectroscopy,

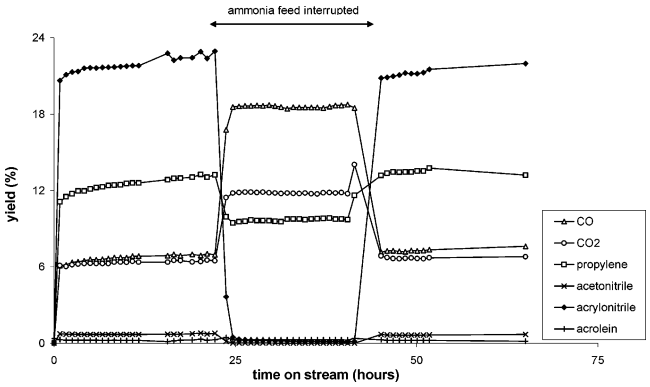

Figure 7. Yields to different products versus time on-stream (TOS). Reaction conditions: total flow, 20 mL/min; feed composition (% volume), $C_2H_8/O_2/NH_3$ (9.8/25/8.6), 200 mg of catalyst. Reaction temperature: 500 °C.

but $SbVO_4$ domains must be better defined after reaction, because its diffraction pattern is not visible in the fresh sample. This is consistent with previous studies that show a more extensive formation of $SbVO_4$ during propane ammoxidation.[13,16,36,37] The XPS quantitative analysis of the surface of the catalyst (Table 1) indicate that the Sb/V atomic ratio is the same as the bulk one, differing from results of other Sb−V-containing systems where a significant Sb[1,16,23−25] or V[13] surface enrichment is reported. An equal composition at the surface and in the bulk can be obtained in supported Sb−V oxides by using methods that provide a homogeneous cation distribution in the deposited oxide.[23] The use of a solid-state synthesis method may also result in a surface composition equal to the bulk one.[13] The atomic Sb/V ratio does not change during reaction, unlike most V−Sb−O catalysts prepared by the slurry methods, which exhibit an increase[13,18,34] or a decrease[16] of the Sb/V atomic ratio. However, when the preparation method affords a more efficient Sb−V interaction, the XPS Sb/V atomic ratio shows little variation, if any, upon use in reaction.[23,38,39] The preparation method used here with soluble V and Sb precursors promoted the Sb−V interaction, and the characterization of the fresh catalyst shows no segregated Sb oxide phases, and this situation is maintained after reaction; from this perspective, the use of this method provides clear advantages over the solid-state synthesis, mainly due to a more efficient V−Sb interaction during the preparation. In line with works reporting an efficient Sb−V interaction during the synthesis, no appreciable change in the Sb/V XPS atomic ratio is reported. However, the Al/(Sb + V) surface ratio (Table 1) decreases after reaction, evidencing a redistribution of the $SbVO_4$ phase in the surface of the alumina occurs during reaction, producing a better exposure of the active sites. Raman and XPS spectra show no change in the nature of the Sb−V−O system during reaction. The preparation method in this sample uses a soluble precursor of antimony (tartrate), which allows for a more close interaction with the soluble vanadium precursor.[28,40] Therefore, Sb−V interaction in this fresh catalyst is higher than that during preparations that do not use dissolved precursors. This trend is in accordance with XPS and ISS studies of Sb−V−O catalysts prepared by the slurry and by solid-state reaction methods.[13] If the preparation affords an efficient Sb−V interaction, ammoxidation reaction does not provide significant additional Sb−V interaction; thus, there is no appreciable transformation during reaction in the catalysts prepared by solid-state reaction[13] or from soluble precursors (this work), while the samples prepared by the slurry method show a larger fraction of segregated phases that further interact during ammoxidation reaction.[13,16,41] The oxidation states in $SbVO_4$ are determined as Sb^{5+} and V^{3+} by Mössbauer[13,42] and EPR spectroscopy.[43] The reduction to V^{3+} is partially reversible since a vanadium-dispersed species appears again on the surface of catalysts under oxidizing conditions.[40,37] This must account for the presence of surface VO_x species (Raman band near 1024 cm^{-1}) is present in the spectrum of used catalyst, because this spectrum has been taken under synthetic air atmosphere at 200 °C. XPS characterization of $VSbO_4$ shows oxidation of surface vanadium species to V^{5+}. These surface V^{5+} species should be in equilibrium with bulk V^{3+} species.

Scheme 1. Reactions Involved in the Formation of Principal Reaction Products

$$C_3H_8 + 1/2O_2 \rightarrow C_3H_6 + H_2O$$
$$C_3H_6 + NH_3 + 3/2O_2 \rightarrow C_3H_3N + 3H_2O \quad \text{(main route)}$$
$$C_3H_8 + NH_3 + 3O_2 \rightarrow C_2H_3N + CO_2 + 4H_2O$$
$$C_3H_8 + 3/2O_2 \rightarrow C_3H_4O + 2H_2O$$

Reaction Network. According to Figure 5, olefinic and oxygenated reaction intermediates appear to be the primary products, which is in line with the reported kinetic reaction network for propane ammoxidation.[5,9,44] The selectivity trend allows one to draw the following conclusions; (i) Propylene, acetonitrile, and acrolein must be primary products, but the yields to acetonitrile and acrolein are very poor; thus, propylene is the main intermediate. (ii) Acrylonitrile is a secondary product that originates from the intermediate propylene. (iii) CO_x are primary and secondary products that are formed from propane and from other reaction products. Therefore, it does appear that acrylonitrile would originate from propylene intermediate. Acrolein is produced to a much lower extent than propylene. Acrolein also appears to be another precursor for acrylonitrile,[21,22,44,45] mainly at low ammonia concentrations.[44] Thus, CO and CO_2 are terminal products and acrylonitrile is a secondary product that originates predominantly from intermediate propylene.[1,5] Scheme 1 shows the reactions involved in the formation of principal reaction products according to these conclusions.

The selectivity−conversion profiles strongly depend on the reaction temperature (Figure 5). When the temperature increases from 420 to 460 °C, the selectivity to acrylonitrile increases, the selectivity to CO_x decreases, and the selectivity to propylene is not significantly affected. The little dependence of propylene selectivity on reaction temperature has already been reported.[9] It has also been underlined that as the reaction temperature increases, the side reaction of ammonia to nitrogen has a detrimental effect on acrylonitrile production, which is particularly intense if the reactor possesses void volume[46,47] or in the case of stainless steel reactors.[9] The present study is run in quartz reactors with minimized void volume, where the gas-phase contribution is negligible.[28] Thus, a moderate increase in the reaction temperature affords an increase in acrylonitrile selectivity similar to that previously reported.[9]

When propane partial pressure is increased, the yield to acrylonitrile decreases linearly and the yield to propylene remains constant (Figure 6A). This trend can be explained by taking into account that as propane concentration increases, the availability of ammonia for ammoxidation becomes limited. The yields to carbon oxides show a moderate decrease with propane partial pressure. The yields to acetonitrile and acrolein increase with propane partial pressure, but they are minor products. Acrylonitrile is the main product up to 10% propane concentration, just below the explosion limit.[9]

The effect of ammonia on selectivity (Figure 6B) can be understood according to a competitive adsorption between NH_3

and O_2.[9] The competition of NH_3 and O_2 on vanadia sites has also been observed by IR on alumina-supported vanadia.[40] Adsorbed ammonia species would minimize the formation of reactive surface oxygen species arising from molecular oxygen adsorption.[41] The increase of CO_2 with oxygen concentration (Figure 6C) is due to the competitive adsorption of ammonia and oxygen[9,44] that affords highly reactive surface oxygen species. The role of oxygen is to keep the oxidation state of the catalyst, since transient pulse studies show that the lattice oxygen participates in the reaction pathway over V−Sb−O catalysts.[19] This accounts for the need to use a low oxygen feed.[9] The competitive adsorption of NH_3 and O_2 must account for the reduction of the surface vanadium oxide species during ammoxidation reaction if compared with ODH reaction conditions.[33,48]

The use of soluble Sb and V precursos maximizes the Sb−V interaction; thus, this sample may not undergo additional Sb−V entanglement during reaction, which is consistent with the Raman spectra of the fresh and used catalysts. In the absence of ammonia, combustion and propane oxidative dehydrogenation are the main reactions (Figure 7). When ammonia feed is restored, the yields to all the products return to the values prior to ammonia cutoff. The shift to propylene and CO_x upon ammonia cutoff is in line with the competitive adsorption of NH_3 and O_2.[9,44] The quick return to steady-state ammoxidation on restoring ammonia feed suggests that the transient catalytic operation must be due to a structural change during the first hours. The initial increase of acrylonitrile formation does not appear related to a change in the chemical nature of the active phase; the Raman spectra show no transformation in the nature of the $SbVO_4$ phase. However, the XPS decrease of the Al/(Sb + V) ratio upon use in reaction indicates a better coverage of alumina support by $SbVO_4$, thus affording higher exposure of the $SbVO_4$ sites. This redistribution must account for the initial transient activation of the catalyst and the generation of an X-ray diffraction pattern.

Nature of the Active Sites. The first step in the propane ammoxidation is the hydrogen abstraction, be it primary or secondary. Pulse experiments on $Sb-V-O/Al_2O_3$ catalysts with selectively deuterated propane[38] have concluded that the abstraction of secondary hydrogens occurs 12−14 times faster than the abstraction of primary hydrogens. But studies with Ga- and Sb-based catalysts[7] have concluded that the first step in the propane ammoxidation is a primary hydrogen abstraction. Both routes could be possible, and the fact that one route could be more favored that the other depends on the reaction temperature and on the specific catalyst.[49] However, isotopic labeling during propane oxidative dehydrogenation on alumina-supported vanadia showed that the abstraction of the secondary H is the rate-determining step.[14] Thus, it appears that, in $Sb-V-O/Al_2O_3$ catalysts, exposed vanadium sites must account for the activation of hydrocarbon. This is the accepted understanding.[1,50] Vanadium is a major component in the formulation of catalyst for selective oxidation reactions.[51−55] This is also in line with several works that studied how the activity of the catalyst decreases as the vanadium content is decreased[56] or when vanadium is substituted by titanium.[57] Still, a debate remains about the exact V functionality that activates propane (terminal V═O or bridging oxygen species connected to V). To the best of our knowledge, no conclusive evidence has been reported for propane ammoxidation. However, the initial activation of propane by vanadium is toward propylene.[9,14,18,44,57−59] For alkane oxidative dehydrogenation, it has been shown that the terminal V═O bond must be ruled out for oxidative dehydrogenation reactions[31,51] of ethane,[39,60] propane[61,62] and butane.[54,63] Thus, the active functionality must be a bridging oxygen connected to surface vanadium sites. *Operando* Raman-GC studies (i.e., simultaneous reaction in situ Raman spectroscopy and on-line catalytic measurement in a single experiment) illustrate that the presence of surface vanadia species proves critical to significantly increase total yield values to acrylonitrile and the specific rate of acrylonitrile formation per vanadium site.[28,48] But an increase in V/Sb ratio shifts the reaction pathway to oxidative dehydrogenation and nonselective oxidation.[58,59,64,65] Thus, V sites promote propane activation, but need the cooperation of another site or phase to afford N-insertion.

Vanadium sites are involved in the activation of propane, and antimony sites should be involve in the selectivity toward acrylonitrile, in the insertion of N in the propylene intermediate molecule. So, the best acrylonitrile yields have been achieved for catalysts with Sb/V near 1.[18,26,58,59,64,65]

Conclusions

Propane ammoxidation on alumina-supported $SbVO_4$ exhibited a transient activation. Unlike other catalysts made with other preparation methods, this transient activity is not due to a change in the nature of the phase, but to a better exposure of the $SbVO_4$ phase. In line with previous works, the ammoxidation of propane to acrylonitrile proceeds via propylene intermediate and, to a lesser extent, via acrolein intermediate. As in propane oxidative dehydrogenation on vanadia catalysts, the V═O functionality does not appear to be the critical sites for propane activation. Such activation may be due to the V−O−Sb functionality, which may also provide the right configuration of acrylonitrile formation.

Acknowledgment

This research was funded by CICYT, Spain, under Project MAT2002-0400-C02-01 and the Spanish Ministry of Education and Science, Project CTQ2005-02802/PPQ. We thank Dr. M. A. Vicente, from Salamanca University (Spain), for the XRD measurements and his helpful comments. M.O.G.-P. thanks the Ministry of Science and Technology, Spain, for a doctorate studies fellowship.

Literature Cited

(1) Grasselli, R. K. In *Handbook in Catalysis*; Ertl, et al., Eds.; Wiley-VCH: Weinheim, Germany, 1997; Vol. V, p 2302.

(2) Brazdil, J. F. *Encyclopedia of Chemical Technology*; Kirk-Othmer Encyclopedia; Wiley-Interscience: New York, 1991.

(3) Grasselli, R. K. *Top. Catal.* **2002**, *21*, 79.

(4) *Chem. Week* **1997**, *159* (June 4), 5.

(5) Catani, R.; Centi, G.; Trifirò, F.; Grasselli, R. K. *Ind. Eng. Chem. Res.* **1992**, *31*, 107.

(6) Bowker, M.; Bicknell, C. R.; Kerwin, P. *Appl. Catal., A* **1996**, *136*, 205.

(7) Sokolovskii, V. D.; Davydov, A. A.; Ovsitser, O. Y. *Catal. Rev.* **1995**, *37*, 425.

(8) Kim, Y. C.; Ueda, W.; Moro-Oka, Y. *Appl. Catal., A* **1991**, *70*, 189.

(9) Centi, G.; Grasselli, R. K.; Trifirò, F. *Catal. Today* **1992**, *13*, 661.

(10) Brazdil, J. F.; Bartek, J. P. U.S. Patent 5,854,172, 1998. Brazdil, J. F.; Kobarvkantei, F. A. P.; Padolwski, J. P. JP Patent 11033399, 1999. Guttmann, A. T.; Grasselli, R. K.; Brazdil, F. J. U.S. Patents 4,746,641, 4,788,173, and 4,837,233, 1998. Brazdil, J. F.; Cavalcanti, F. A. P. EP Patent 0765684, 1997. Cavalcanti, F. A. P.; Bremer, N. L.; Brazdil, L. C. WO Patent 9505895, 1995.

(11) Grasselli, R. K. *Catal. Today* **1999**, *49*, 141.

(12) Andersson, S. L. T.; Andersson, G.; Centi, R. K.; Grasselli, M.; Sanati, F.; Trifirò, F. *Stud. Surf. Sci. Catal.* **1993**, *75*, 691.

(13) Zanthoff, H. W.; Grünert, W.; Buchholz, S.; Heber, M.; Stievano, L.; Wagner, F.; Wolf, G. *J. Mol. Catal. A* **2000**, *162*, 443.

(14) Chen, K.; Khodakov, A.; Yang, J.; Bell, A. T.; Iglesia, E. *J. Catal.* **1999**, *186*, 325.
(15) Nilsson, J.; Landa-Cánovas, A. R.; Hansen, S.; Andersson, A. *J. Catal*. **1996**, *160*, 244.
(16) Nilsson, J.; Landa-Cánovas, A. R.; Hansen, S.; Andersson, A. *J. Catal*. **1999**, *186*, 442.
(17) Ratajczak, O.; Zanthoff, H. W.; Geisler, S. *Stud. Surf. Sci. Catal*. **2000**, *130*, 1685.
(18) Guerrero-Pérez, M. O.; Fierro, J. L. G.; Vicente, M. A.; Bañares, M. A. *J. Catal.* **2002**, *206*, 339.
(19) Zanthoff, H. W.; Buchholz, S. *Catal. Lett*. **1997**, *49*, 213.
(20) Albonetti, S.; Blanchard, G.; Buratin, P.; Cassidy, T. J.; Masetti, S.; Trifirò, F. *Catal. Lett*. **1997**, *45*, 119.
(21) Zanthoff, H. W.; Buchholz, S. *Heterogeneous Hydrocarbon Oxidation*; ACS Symposium Series 638; American Chemical Society: Washington, DC, 1996; Chapter 19. Buchholz, S. A.; Zanthoff, H. W. *Heterogeneous Hydrocarbon Oxidation*; ACS Symposium Series 638; American Chemical Society: Washington, DC, 1996; Chapter 41, p 210.
(22) Centi, G.; Marchi, F. *Stud. Surf. Sci. Catal*. **1996**, *101*, 277.
(23) Vislovskiy, V. P.; Shamilov, N. T.; Sardarly, A. M.; Vichkov, V. Y.; Sinev, M. Y.; Ruiz, P.; Valenzuela, R. X.; Cortés-Corberán, V. *Chem. Eng.* **2003**, *95*, 37.
(24) Barbaro, S.; Larrondo, S.; Duhalde, N.; Amadeo, N. *Appl. Catal., A* **2000**, *193*, 277.
(25) Larrondo, S.; Irigoyen, B.; Baronetti, G.; Amadeo, N. *Appl. Catal., A* **2003**, *250*, 279.
(26) Guerrero-Pérez, M. O.; Fierro, J. L. G.; Bañares, M. A. *Phys. Chem. Chem. Phys.* **2003**, *5*, 4032.
(27) Guerrero-Pérez, M. O.; Fierro, J. L. G.; Bañares, M. A. *Catal. Today* **2003**, *78*, 387.
(28) Guerrero-Pérez, M. O.; Bañares, M. A. *Catal. Today* **2004**, *96*, 265.
(29) Wagner, C. D.; Davis, L. E.; Zeller, M. V.; Taylor, J. A.; Raymond, R. H.; Gale, L. H. *Surf. Interface Anal*. **1981**, *3*, 211.
(30) Guerrero-Pérez, M. O. Ph.D. Dissertation, Universidad Autónoma de Madrid, Spain, 2003.
(31) Bañares, M. A.; Wachs, I. E. *J. Raman Spectrosc.* **2002**, *33*, 359.
(32) Vedrine, J. C.; Novakova, E. K.; Derouane, E. G. *Catal. Today* **2003**, *81*, 247.
(33) Poulston, S.; Price, N. J.; Weeks, C.; Allen, M. D.; Parlett, P.; Steinberg, M.; Bowker, M. *J. Catal*. **1998**, *178*, 658.
(34) Aït-Lachgar-Ben Abdelouabad, K.; Roullet, M.; Brun, M.; Burrows, A.; Kiely, C. J.; Volta, J. C.; Abon, M. *Appl. Catal., A* **2001**, *210*, 121.
(35) Berry, F. J.; Brett, M. E.; Patterson, W. R. *J. Chem. Soc., Dalton Trans.* **1983**, 9.
(36) Centi, G.; Foresti, E.; Guarnieri, F. *Stud. Surf. Sci. Catal*. **1994**, *82*, 281.
(37) Guerrero-Pérez, M. O.; Bañares, M. A. *Chem. Commun*. **2002**, 1292.
(38) Brazdil, L. C.; Ebner A. M.; Brazdil, J. F. *J. Catal*. **1996**, *163*, 117.
(39) Bañares, M. A.; Martínez-Huerta, M. V.; Gao, X.; Wachs, I. E.; Fierro, J. L. G. *Stud. Surf. Sci. Catal*. **2000**, *130A*, 3125.
(40) Sobalik, Z.; Kozlowski, R.; Haber, J. *J. Catal*. **1991**, *127*, 665.
(41) Centi, G.; Perathoner, S. *Appl. Catal., A* **1995**, *124*, 317.
(42) Birchall, T.; Sleight, A. W. *Inorg. Chem*. **1976**, *15*, 868.
(43) Berry, F. J.; Brett, M. E. *Inorg. Chim. Acta* **1983**, *7*, L205.
(44) Sanati, M.; Akbari, R.; Masetti, S.; Trifirò, F. *Catal. Today* **1998**, *42*, 325.
(45) Nilsson, R.; Lindblad, L.; Andersson, A. *Catal. Lett*. **1994**, *29*, 409.
(46) Kim, Y. C.; Ueda, W.; Moro-Oka, Y. *Catal. Today* **1992**, *13*, 673.
(47) Kim, Y. C.; Ueda, W.; Moro-Oka, Y. *Appl. Catal.* **1991**, *70*, 189.
(48) Bañares, M. A.; Guerrero-Pérez, M. O.; Fierro, J. L. G.; Cortez, G. G. *J. Mater. Chem*. **2002**, *12*, 3337.
(49) Bettahar, M. M.; Costentin, G.; Savary L.; Lavalley, J. C. *Appl. Catal*. **1996**, *145*, 1.
(50) Grasselli, R. K.; Burrington, J. D.; Buttrey, D. J.; DeSanto Jo, P.; Lugmair, C. G.; Volpe, A. F., Jr.; Weingand, T. *Top. Catal*. **2003**, *23*, 5.
(51) Bañares, M. A. *Catal. Today* **1999**, *51*, 319.
(52) Blasco, T.; López Nieto, J. M. *Appl. Catal., A*. **1997**, *157*, 117.
(53) Mamedov, E. A.; Cortés Corberán, V. *Appl. Catal., A* **1995**, *127*, 1.
(54) Wachs, I. E.; Jehng, J. M.; Deo, G.; Weckhuysen, B. M.; Guliants, V. V.; Bezinger, J. B.; Sundaresan, S. J. *J. Catal*. **1997**, *170*, 75.
(55) Guliants, V. V. *Catal. Today* **1999**, *51*, 255.
(56) Derouane-Abd Hamid, S. B.; Centi, G.; Pal, P.; Derouane, E. G. *Top. Catal.* **2001**, *15*, 161.
(57) Wickman, L. R.; Wallenberg, A.; Andersson, A. *J. Catal*. **2000**, *194*, 153.
(58) Nilsson, R.; Lindblad, T.; Andersson, A.; Song, C.; Hansen, S. *Stud. Surf. Sci. Catal*. **1994**, *82*, 293.
(59) Andersson, S. L. T.; Andersson, A.; Centi, G.; Grasselli, R. K.; Sanati, M.; Trifirò, F. *Appl. Catal., A* **1994**, *113*, 42.
(60) Bañares, M. A.; Gao, X.; Fierro, J. L. G.; Wachs, I. E. *Stud. Surf. Sci. Catal*. **1997**, *107*, 295.
(61) Garcia Cortez, G.; Bañares, M. A. *J. Catal*. **2002**, *209*, 197.
(62) Garcia Cortez, G.; Fierro, J. L. G.; Bañares, M. A. *Catal. Today* **2003**, *78*, 219.
(63) Wachs, I. E.; Jehng, J. M.; Deo, G.; Weckhuysen, B. M.; Guliants, V. V.; Bezinger, J. B. *Catal. Today* **1996**, *32*, 47.
(64) Andersson, S.; Hansen, A.; Wickman, *Top. Catal.* **2001**, *15*, 103.
(65) Centi, G.; Perathoner, S.; Trifirò, F. *Appl. Catal., A* **1997**, *157*, 14.

Received for review September 7, 2005
Revised manuscript received April 6, 2006
Accepted April 19, 2006

IE051000G